International Journal of Innovative
Computing, Information and Control
Volume 8, Number 12, December 2012

 ISSN 1349-4198
pp. 8133–8145

TIME DELAY COMPENSATED VISION BASED STABILIZATION CONTROL OF AN INVERTED PENDULUM

Selcuk Kizir, Hasan Ocak, Zafer Bingul and Cuneyt Oysu

Department of Mechatronics Engineering
Kocaeli University
Umuttepe Campus, Kocaeli 41380, Turkey
{ selcuk.kizir; hocak; zaferb; coysu }@kocaeli.edu.tr

Received September 2011; revised January 2012

Abstract. *In this study, vision based stabilization control of a real time cart-pole inverted pendulum system was implemented. Inverted pendulum system is one of the classical problems and most widely used experimental setups in control theory. The pendulum angle and cart position were measured using a camera instead of encoders. A graphical user interface (GUI) was developed in Visual Basic for image processing. Visual markers were not used to aid the algorithm in detecting the pendulum angle and the cart position from the camera images. The image processing algorithm was robustly designed against visual disturbances which enter the field of view of the camera. The time delay in measurements that arises in the image processing part of the system was reduced with an effective prediction algorithm. Full state feedback method was used to stabilize the pendulum system. The control algorithms were implemented in Simulink® environment and embedded in Dspace DS1103 real time controller. The system was proven to be robust to visual and physical (external force) disturbances. The image processing algorithm was able to process 50 frames per second (fps) with an average of 35ms total time delay and the cart position and the pendulum angle were obtained with 0.86mm and 0.1° resolution, respectively.*

Keywords: Inverted pendulum, State feedback, Time delay, Visual feedback

1. **Introduction.** Inverted pendulum system is one of the most widely used experimental setups in the control systems because it has a simple structure and it is a nonlinear and an unstable system [1-9]. Various inverted pendulum systems with different structures were developed and controlled in the literature: single and double rod cart-pole [1-6], single and double rod rotary [7], 2 DOF [8], mobile [9], parallel and coupled with a serial robot inverted pendulum systems.

One of the significant aspects of an inverted pendulum system is that the system represents the basis for many complex systems such as dynamics of a robotic arm, standing human model, rockets, motorized transport devices, satellite control and landing systems of aircrafts. The examples can be illustrated as shown in Figure 1. Therefore, the inverted pendulum system is accepted as one of the benchmark experimental setups in the control systems field.

In an inverted pendulum system, the rod is attached to a cart which can move through a limited horizontal track via a motor. Generally, pendulum angle and cart position are measured via incremental encoders. Other state variables like speed and acceleration are also computed from measured encoder outputs in the controller.

An inverted pendulum system has two control problems. The first one is called the swing-up or the stand-up and the second one is the stabilization problem. For the swing-up problem, the pendulum has to be brought in to its inverted position from its lower stable equilibrium point or any other position to its upper unstable equilibrium point

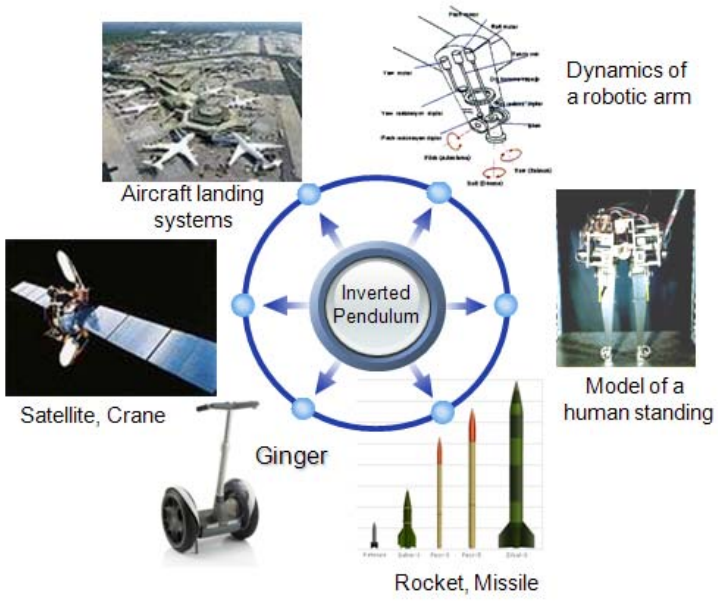

FIGURE 1. Some examples related to inverted pendulum system

where the stabilization controller is switched on. The main control problem for an inverted pendulum system is the stabilization problem which consists of keeping the pendulum in its equilibrium point while maintaining the cart at a desired position. Detailed information about inverted pendulum systems can be found in [2]. In this study, the second control problem was explored. The system was controlled using a linear quadratic regulator (LQR) based full state feedback control method.

In the literature, there are several studies about vision based control of an inverted pendulum system. These studies have some drawbacks such as the usage of visual markers helping to detect the cart and the rod from the camera images, low resolutions for pendulum angle and the cart position, measuring only pendulum angle while using an encoder for the cart position, large oscillations around the unstable equilibrium point of the pendulum and a large time delay. Magana and Holzapfel [3] controlled only the pendulum angle with a vision based fuzzy logic controller but the continuous oscillations in the pendulum angle at rest were about $\pm 2.7^\circ$. Espinoza-Quesada and Ramos-Velasco [4] studied vision based control of an inverted pendulum with a full state feedback using a DSP. The total oscillation at rest position was about $\pm 10^\circ$ for the pendulum angle and ± 0.2m for the cart position. Similarly, Tu and Ho [7] controlled a rotary pendulum using a system based on FPGA and DSP with visual feedback. Only, the pendulum angle was measured and a visual marker was used for detecting the rod. Based on the results provided in the study, the pendulum and the arm angles were controlled within $\pm 1.5^\circ$ and $\pm 5^\circ$, respectively. Wang et al. [5] used a camera to measure the pendulum angle and an incremental encoder for the cart position. They explored the two control problems of the inverted pendulum system. They used the bang-bang algorithm for the swing-up problem and proposed two loops stabilization (observer based linearization and Lyapunov based controller) control algorithm. The swing-up response was not provided in their study. Under the stabilization control, the pendulum angle and the cart position were oscillating about $\pm 10^\circ$ and ± 0.04m continuously. Similar studies can also be found in the literature [6,8].

In this study, both the cart position and the pendulum angle were determined based on vision feedback. The proposed image processing algorithm is superior to others in the

literature in many ways. Visual markers were not used to make the localization of the cart and the rod straightforward. In addition, the algorithm was designed robust to visual disturbances. These disturbances can be another object or a person moving within the field of view of the camera without getting in front of the cart or the rod so the view is not totally lost. The processing time of the algorithm is only about 20ms. Acquiring a frame from the camera, sending it via USB, processing the frame and sending the variables (cart position and pendulum angle) via RS232 take an average of 60ms. The 60ms time imposed on the system as delay was reduced to 35ms through an effective estimation algorithm. The applied time delay compensation increased the robustness of the system. The image processing algorithm also provided high resolutions for the cart position and the pendulum angle: 0.86mm for the cart position and 0.1° for the pendulum angle. A comparison table is also provided in the Results section which compares the proposed scheme with the existing studies in several aspects.

2. **Inverted Pendulum System.** The system consists of several parts such as a servo motor in order to provide movement of the cart and to apply the desired force to the pendulum, a servo motor driver in speed control mode, a camera in order to measure the state variables: cart position (p) and pendulum angle (θ), two incremental encoders in order to compare measurements, a PC for image processing and a real time controller in order to apply the control methods. The experimental setup is shown in Figure 2. The developed control algorithm runs on a powerful rapid control prototyping board, dSPACE DS1103.

State space model of the system. Model parameters and state space model of the system is given in Table 1.

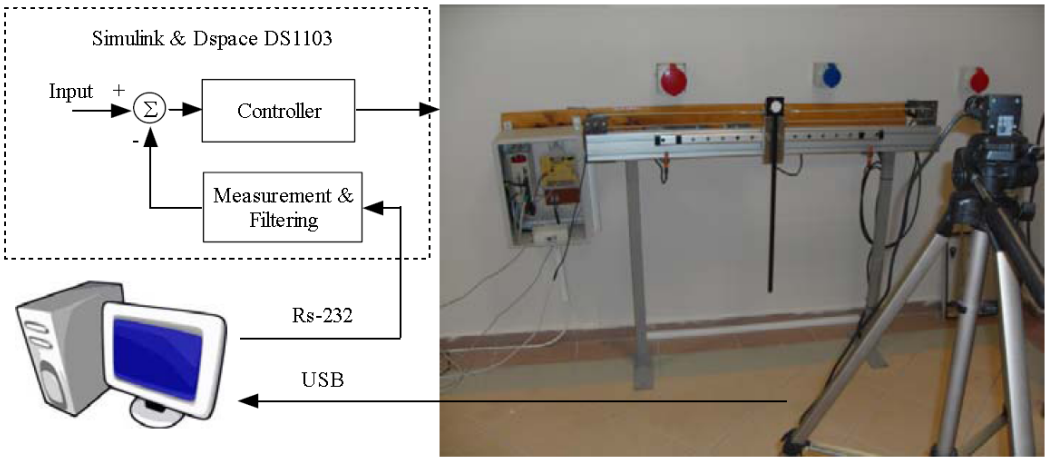

FIGURE 2. Setup for the vision based cart pole inverted pendulum system

TABLE 1. Model parameters for the inverted pendulum system

g	Gravitational acceleration: $g = 9.81\text{m/s}^2$
m	Mass of the pendulum: $m = 0.2\text{kg}$
M	Mass of the cart: $M = 1.095\text{kg}$
l	Length to pendulum center of mass: $l = 0.325\text{m}$
b	Viscous damping coefficient between rod and cart: $b = 0.001\text{N/rad/sn}$
c	Viscous damping coefficient between cart and surface: $c = 0.001\text{N/m/sn}$
I	Inertia: $I = 0$

$$\dot{\mathbf{x}} = \mathbf{A}\mathbf{x} + \mathbf{B}u \tag{1}$$

$$\mathbf{x} = \begin{pmatrix} x_1 \\ x_2 \\ x_3 \\ x_4 \end{pmatrix} = \begin{pmatrix} p \\ \dot{p} \\ \theta \\ \dot{\theta} \end{pmatrix} \tag{2}$$

$$\dot{\mathbf{x}} = \begin{bmatrix} 0 & 1 & 0 & 0 \\ 0 & -c/M & -mg/M & b/Ml \\ 0 & 0 & 0 & 1 \\ 0 & c/Ml & (M+m)g/Ml & -(m+M)b/Mml^2 \end{bmatrix} \begin{pmatrix} x_1 \\ x_2 \\ x_3 \\ x_4 \end{pmatrix} + \begin{bmatrix} 0 \\ 1/M \\ 0 \\ -1/Ml \end{bmatrix} u \tag{3}$$

3. **Controller.** The stabilization of the pendulum and keeping the cart in its desired position is aimed in this study. In order to realize this aim, full state feedback control method is applied to the pendulum system.

In order to place the closed loop poles to desired locations in the s-plane, state vector $\mathbf{x}$ is multiplied by a gain vector $\mathbf{K}$ and the result is fed back to the control signal u.

$$\begin{aligned} \dot{\mathbf{x}} &= \mathbf{A}\mathbf{x} + \mathbf{B}u \\ \mathbf{y} &= \mathbf{C}\mathbf{x} \end{aligned} \tag{4}$$

State equations of the closed loop system are given in Equation (5) [10]. Thus, the system poles given by the eigen-values of the state transition matrix $\mathbf{A}$ are now determined by $\mathbf{A} - \mathbf{BK}$. The gain vector $\mathbf{K}$ is tuned so that the closed-loop system poles are placed to desired locations to achieve required control criteria.

$$\begin{aligned} \dot{\mathbf{x}} &= \mathbf{A}\mathbf{x} + \mathbf{B}u = \mathbf{A}\mathbf{x} + \mathbf{B}(-\mathbf{K}\mathbf{x} + r) = (\mathbf{A} - \mathbf{BK})\mathbf{x} + \mathbf{B}r \\ \mathbf{y} &= \mathbf{C}\mathbf{x} \end{aligned} \tag{5}$$

$$\mathbf{K} = [k_1 k_2 \ldots k_n] \tag{6}$$

The system poles can theoretically be placed to any desired point with a suitable gain vector for any system. Fast and stable system responses can be accomplished using this method. However, the actual performance is limited by the physical hardware. The best results can be achieved by optimizing between control effort and the response time. This can be accomplished numerically using a linear quadratic regulator (LQR) method given by

$$J = \int_0^\infty \mathbf{x}(t)^T \mathbf{Q}\mathbf{x}(t) + u(t)^T R u(t) dt \tag{7}$$

The MATLAB function "LQR" performs this operation and computes the optimum gain vector. This function also allows for weighting of both the state errors and the control effort. The matrix $\mathbf{Q}$, the coefficient R and the gain vector $\mathbf{K}$ as computed by the LQR function of MATLAB software are given below.

$$\mathbf{Q} = \begin{bmatrix} 1 & 0 & 0 & 0 \\ 0 & 10^{-4} & 0 & 0 \\ 0 & 0 & 13 & 0 \\ 0 & 0 & 0 & 10^{-4} \end{bmatrix}, R = 10^{-4} \text{ and } \mathbf{K} = [-100 - 95 - 450 - 48]$$

The main model for the controller was designed in Simulink as depicted in Figure 3. The model has some subsystems such as measurement, camera, filtering, input and controller. The main functions of these subsystems can be listed as: measurement of the cart position and the pendulum angle from the encoders and the camera, the derivation of the cart's velocity and the rod's angular velocity, lowpass filtering of the state variables, obtaining

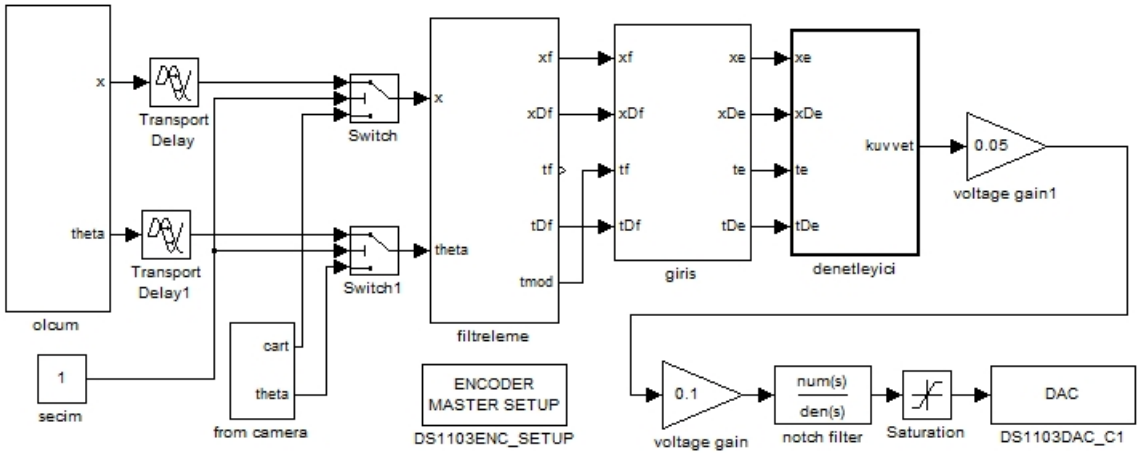

FIGURE 3. The simulink model for the main controller

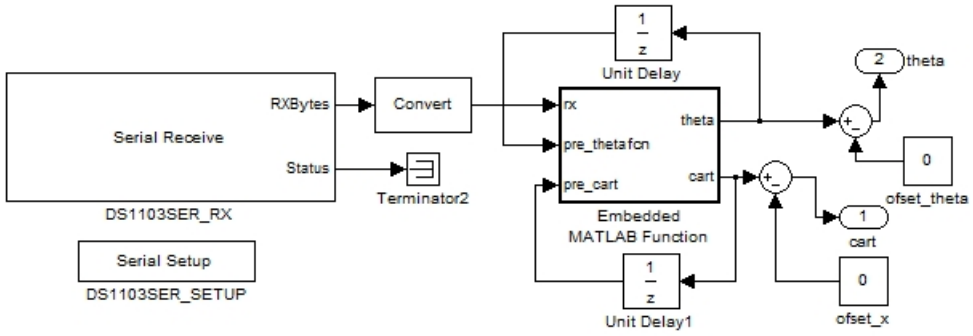

FIGURE 4. Communication with image algorithm subsystem model

the error signals and finally implementation of full state feedback control. The transport delay blocks are also added to outputs of the encoder measurement subsystem in order to determine the critical time delay of the system. According to experimental results, the critical time delay (applied to all variables) was determined as 75ms for the system. The details of the camera subsystem are given in Figure 4. The measurements results of the image processing algorithm running on a PC are sent to the dSPACE board via Rs232 connection running at 38400bps.

4. **Image Processing.** The camera and the image processing algorithm make up the one of the most important components of the system. Detailed information about the camera used, the image processing algorithm and the experimental results are provided in the upcoming sections.

4.1. **Camera system.** The iDS UI-1225LE model camera was used which has a maximum resolution of 752×480 pixels, can capture a maximum of 87 frames per second through USB interface and has a colored CMOS image sensor. An 8mm lens was attached to the camera. The camera was placed and fixed at a distance of 1m from the inverted pendulum system so that the field of view covers the work-spaces of the rod and the cart with a maximum resolution.

4.2. **Methods.** In order to maximize the number of frames processed by the image processing algorithm, the camera was set to function in continuous grabbing mode and the frame rate was set to 87fps. In the continuous grabbing mode, while the image is being processed for obtaining the cart position and the pendulum angle, simultaneously the next frame is being grabbed by the camera. Thus, the delay for acquiring the next image after the current image is processed is minimized. At 87fps frame rate the exposure time is so low (11.5ms) that it would limit the amount of light that falls on the camera image sensor. This would cause the camera to produce low-contrast dark images. Increasing the exposure time would solve this problem; however, this will also increase the amount of time needed for image formation which will increase the time delay in the system. Increased time delay will have negative effects on the robustness and the stability of the system. Therefore, instead of increasing the exposure time, the images acquired by the camera were pre-processed using the camera's built-in edge and contrast enhancement filters.

The image processing algorithm developed for obtaining the cart position and the pendulum angle was implemented in Visual Basic 6.0 environment with a graphical user interface (GUI). The flowchart of the algorithm is illustrated in Figure 5. In the designed GUI, the user is first asked to select the wok-spaces of the cart and the pendulum from an acquired frame using a mouse. The user is then asked to locate and select the cart (in zero position) in its workspace. After the user introduces the cart to the program, an edge image of the cart is obtained using a Sobel filter [11] and this edge image is stored as the model of the cart. This step finalizes the interaction between the program and the user and the images acquired from the camera in continuous grabbing mode are processed in a loop. The steps involved in detecting the position of the cart can be summarized as follows: A sub-image consisting of the user defined workspace of the cart is obtained from the original image. This sub-image is processed using a Sobel filter resulting in an edge image of the cart workspace. Correlation between the cart model and this edge image is computed. The size of the cart as it appears in the image would decrease as it moves away from the camera. Thus, the correlation operation is repeated for different scales of the cart model between 0.8 and 1.2. In the correlation operation, the model is slided over the cart work space edge image. The maximum value of the correlation matrix will occur when the model sits over the cart in the image. The position of the cart can be computed from the correlation matrix as follows.

$$p = p_{\max} \frac{i - N_x/2}{N_x} \tag{8}$$

Here, i is the column index of the maximum value in the correlation matrix, $p_{\max}$ is the horizontal field of view of the camera in meters and N_x is the horizontal resolution of the camera. Camera is placed in a position where the horizontal field of view is 65cm and the horizontal resolution of the camera is 752 pixels. With these settings, the cart position was obtained with a resolution of 0.86mm.

The step involved in detecting the pendulum angle can be summarized as follows: A sub-image consisting of the user defined workspace of the pendulum rod is obtained from the original image. The sub-image is converted to black-and-white image using a threshold. The threshold value was determined to be 75 by analyzing sample images. The black-and-white image is then segmented through connected components labeling algorithm [11]. The components detected are further processed and the center of gravity, width, height and the orientation angle are computed for each component. Since the width and the height of the pendulum rod is known, the components that do not match these (up to certain tolerance) are filtered. For each component that passed through the

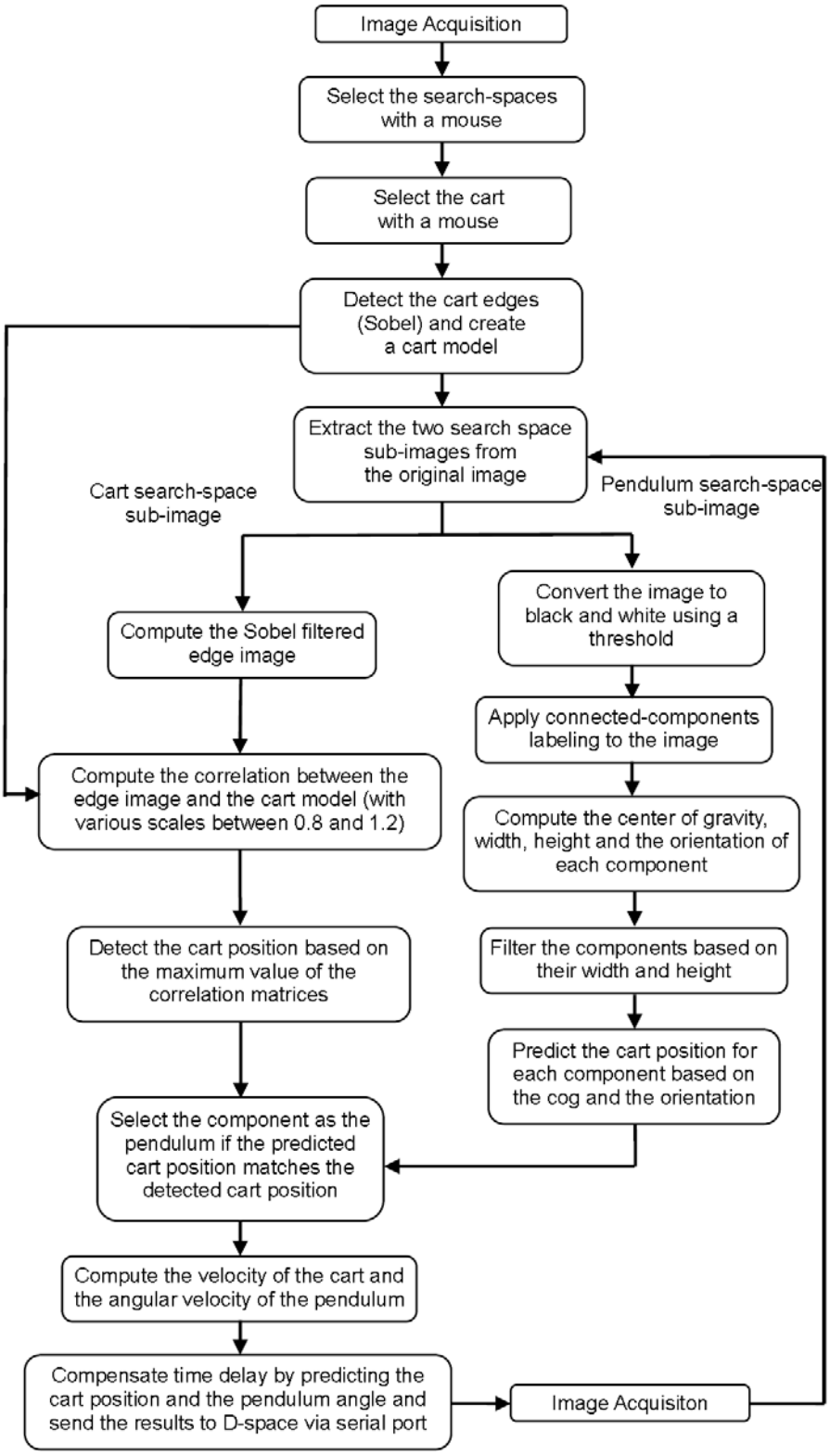

FIGURE 5. The flow-chart of the image processing algorithm

filter, the point where the pendulum rod touches the cart axis is computed from the center of gravity and the orientation angle. Considering that the rod moves freely over the cart, the point computed should be the same as the cart position. The point computed for each component is compared with the actual cart position detected from the sub-image of the

cart workspace. The component providing a correct cart position estimate is selected as the pendulum rod and the orientation angle of this component is determined to be the pendulum angle.

Grabbing of a single frame by the camera, sending it to a PC via USB, processing and sending the cart position and pendulum angle via serial port all together take an average of 60ms. 60ms is approximately divided among various tasks as follows: Grabbing of an image by the camera is 12ms, sending the frame data to a PC via USB is 20ms, processing of the frame is 20ms and sending the processing results (position and angle) via serial port is 8ms. Although, 60ms delay is less than the critical delay of the system, it negatively affects the robustness of the system to disturbances. The time delay of the system was minimized by predicting the cart position and the pendulum angle. The effect of the 60ms delay on the system can be modeled by adding a feedback transfer function block of $e^{-\tau s}$ (τ: time delay) to the system. To eliminate or to reduce the effect of this delay, it would be sufficient to put another transfer function block of $e^{\tau s}$ right after the previous block. However, it is impossible to realize this block since it is an uncausal. As an alternative to this block, one can replace $e^{\tau s}$ with $1 + \tau s$, which is realizable. The output of the new block can be computed as,

$$y = x + \tau \dot{x} \tag{9}$$

This equation can be digitized as,

$$y_k = x_k + \tau \frac{(x_k - x_{k-1})}{t_k - t_{k-1}} \tag{10}$$

In this study, the time delay compensation, τ, was set as $K * t_p$, where t_p is the frame processing time. Since the time delay changes dynamically with the frame processing time, t_p, the amount of time delay compensation was set proportional to the frame processing time. The effect of the prediction gain, K, on the system is studied and the results are provided in the next section.

5. **Results and Discussion.** In order to test the performance of the system, several experiments were conducted. External forces were applied to the rod and visual disturbances were also introduced to the system as the pendulum was stabilized at its equilibrium point.

A graphical user interface (GUI) is designed in Visual Basic 6.0 environment as depicted in Figure 6. In the GUI, the image areas selected by the user are drawn in black

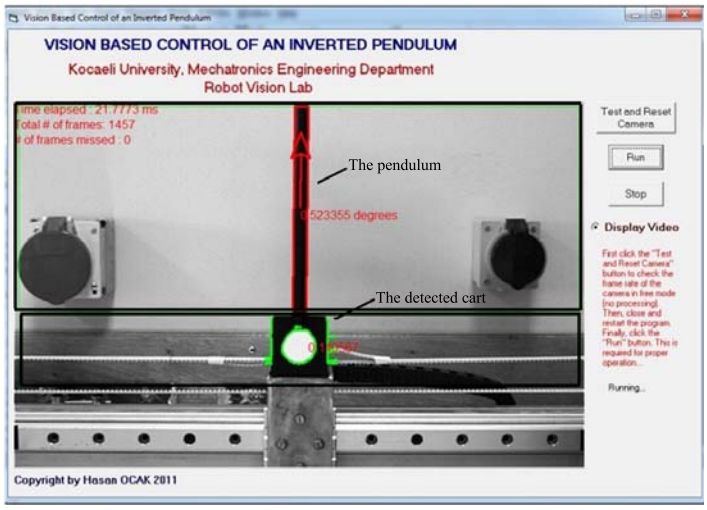

FIGURE 6. A screenshot of the developed GUI

rectangles. The detected cart and the pendulum are shown in Figure 6. The orientation of the pendulum is displayed by an arrow starting from the center of gravity of the rod. Furthermore, the computed cart position and pendulum angle are also displayed on the GUI.

The effect of the prediction gain, K, on the system was analyzed. The experimental results for $K = 0, 1$ are illustrated in Figures 7, 8 and 9, respectively. The upper half of the graph shows the pendulum angle while the lower half shows the cart position. The figures show the measurements obtained from the absolute encoders along with the ones provided by the image processing algorithm. As it can be seen from the figures,

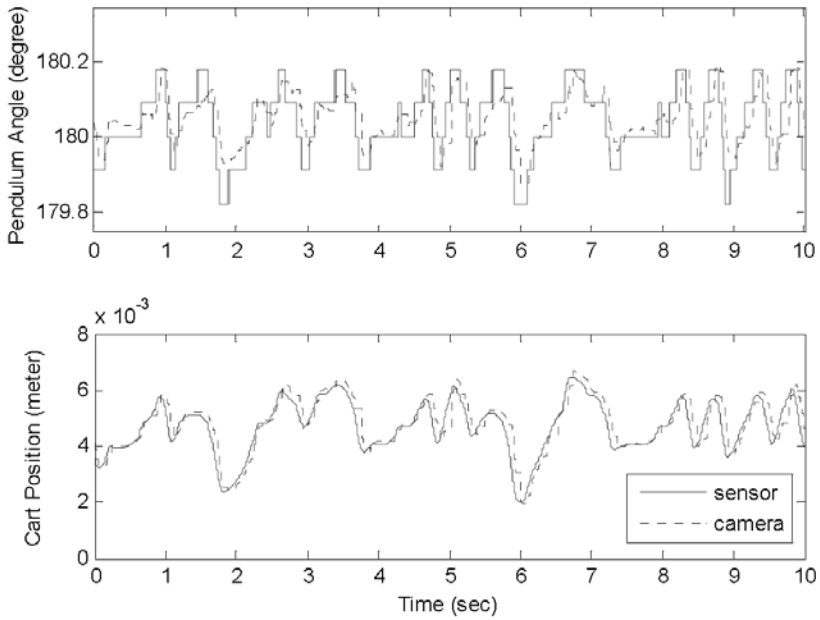

FIGURE 7. System response when $K = 0$ and system was stabilized and at rest

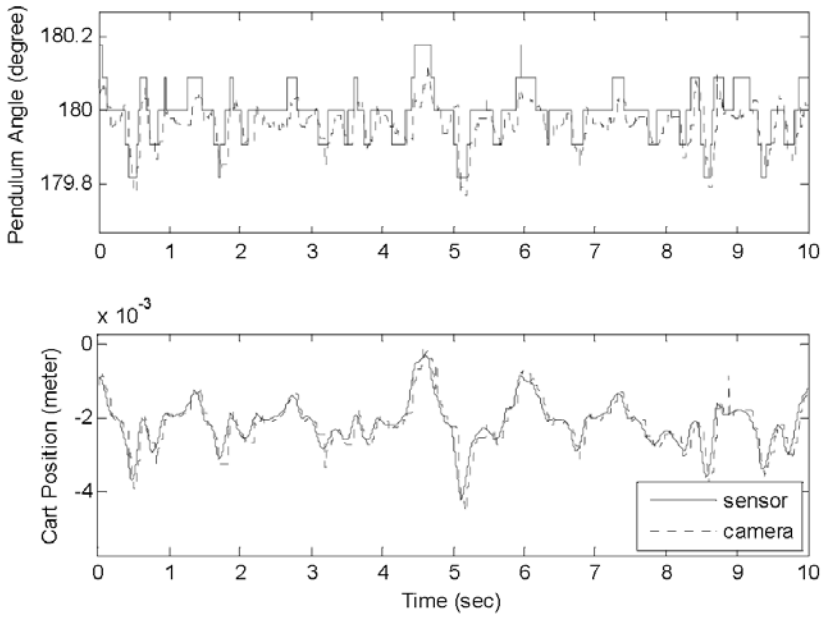

FIGURE 8. System response when $K = 1$ and system was stabilized and at rest

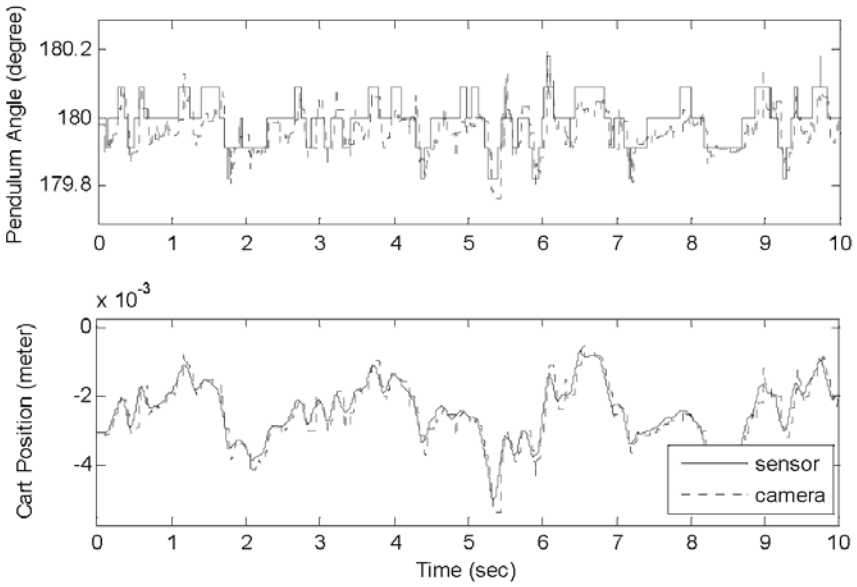

FIGURE 9. System response when $K = 2$ and system was stabilized and at rest

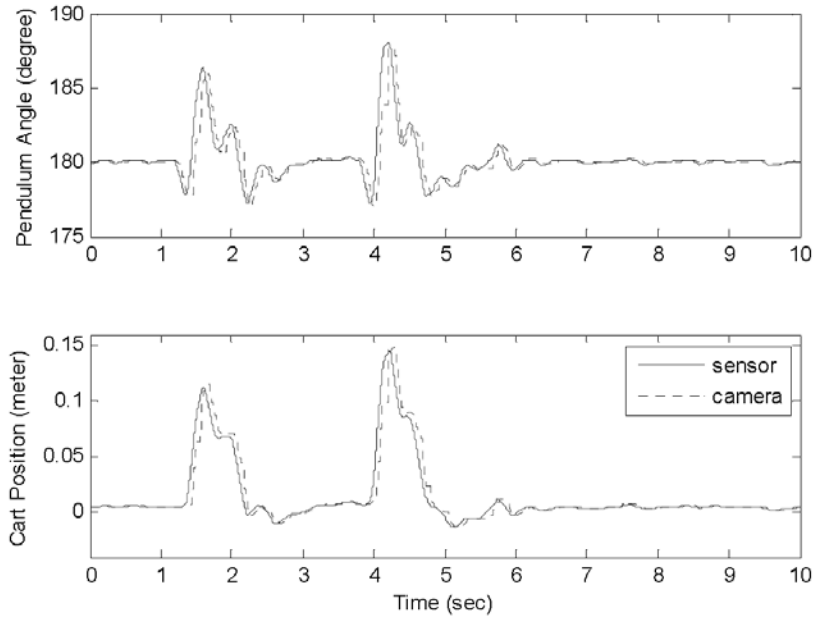

FIGURE 10. System response under external disturbances with $K = 0$

the pendulum angle and the cart position were controlled successfully and they oscillated between only $\pm 0.2^{\circ}$ and ± 0.002m, respectively.

Figures 10 and 11 illustrate the experimental results for different estimation gains under applied external forces in order to loose balance when the system was stabilized and at rest. Both the camera and the encoder measurements are plotted in the figures. As can be seen from the figures, the pendulum angle and the cart position were controlled successfully.

The cross correlation between the measured values for the image processing algorithm and the encoder data is computed in order to see the effects of the estimation algorithm on the time delay. The cross correlation results are shown in Figure 12 for estimation

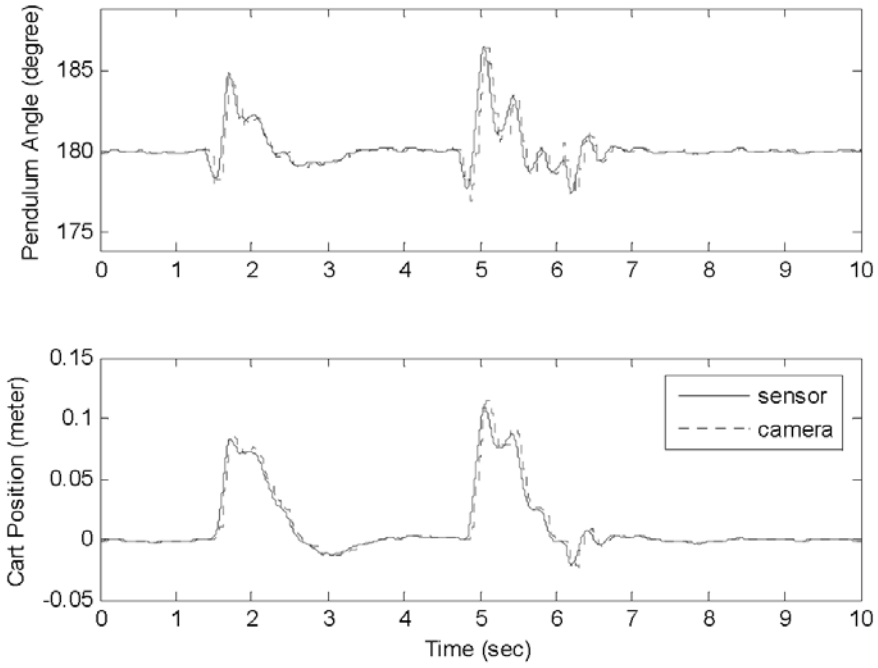

FIGURE 11. System response under external disturbances with $K = 1$

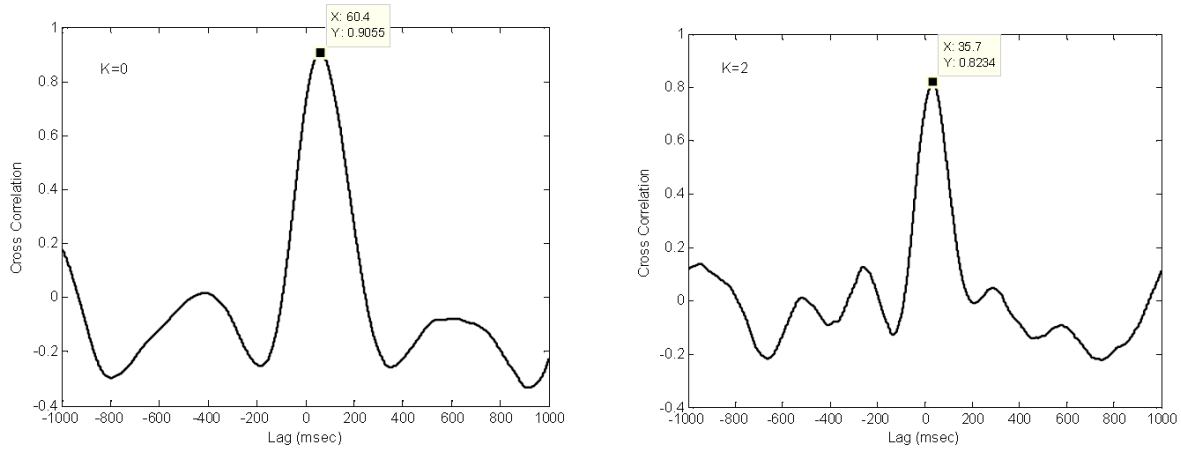

FIGURE 12. Cross correlation plots for $K = 0$ and $K = 2$

TABLE 2. Computed time delays and costs according to estimation gain

Estimation Gain (K)	Time Delay	$\sqrt{\sum e^2}$
0	60.4ms	4.3×10^{-4}
1	39.6ms	3×10^{-4}
2	35.7ms	2.6×10^{-4}

gain $K = 0$ and $K = 2$. The global maximum of the correlation function gives the delay between two measurements.

The time delay and the root mean square (rms) error (between camera and sensor) for different estimation gains were calculated and listed in Table 2 when system was stabilized and at rest. The minimum time delay and error was obtained for $K = 2$. Although increasing estimation gain (K) reduces the time delay, it also negatively affects

TABLE 3. A brief comparison between similar studies

Study	Visual markers	Camera	Estimated state(s)	Estimate resolution	Time delay	Oscillations	Experimental validation
Proposed scheme	×	752 × 480 87fps	Pendulum angle, cart position	0.86mm 0.1°	35ms	±0.002m ±0.2°	✓
Magana and Holzapfel	×	512 × 480 60fps	Pendulum angle	0.25°	25ms	±2.7°	✓
Espinoza-Quesada et al.	×	–	Pendulum angle, cart position	–	–	±0.2m ±10°	✓
Tu and Ho	✓	250fps	Pendulum angle	–	–	±1.5°	✓
Wang et al.	✓	640 × 480 25fps	Pendulum angle	–	> 40ms	±0.04m ±10°	✓

the robustness of the system after some point. This is mainly because the system is very dynamic and the future predictions fail when the pendulum changes direction. Based on the experiments performed, the best values for the estimation gains are found to be between 1 and 2.

The proposed scheme is compared with similar studies in the literature in several aspects: whether the visual markers were used or not, the resolution and the fps of the camera, estimated state(s) (cart position and/or pendulum angle), estimate resolution for both cart position and pendulum angle, time delay imposed on the system, oscillations in cart position and pendulum angle and whether an experimental validation was done or not. The results of the comparison are provided in Table 3. Some of the fields in the table are missing since corresponding data was not made available by the authors of the manuscript. It is clear from the results that the proposed scheme is superior to existing one in several aspects. One can compare the robustness of the methods by analyzing the oscillations in the cart position and the pendulum angle. As provided in the table, the smallest oscillations were obtained for the scheme proposed in this study. In Magana and Holzapfel's study, the time delay imposed on the system is smaller than the proposed scheme. However, the estimate resolution is a lot worse which resulted in larger oscillations thus a less robust scheme. In overall, the results prove that the proposed scheme is superior to existing ones.

The camera used in this study was iDS UI-1225LE model USB 2.0 camera with a maximum resolution of 752 × 480 pixels. USB 2.0 ports have data transfer rates up to 480Mbps. Therefore, the transfer time for a 752 × 480 image from the camera to a PC via USB 2.0 is approximately 20ms. This time is added to the overall time delay of the system which increases the oscillations in both cart position and the pendulum angle. Thus, the robustness of the system is negatively affected. Although, the oscillations for the proposed scheme are very small, it can further be improved by using a USB 3.0 camera. The data transfer rate of a USB 3.0 connection is about 10 times faster than USB 2.0. Therefore, with a similar camera with USB 3.0 interface, the transfer time for an image can be reduced from 20ms to 2ms. This would result in a 18ms time delay improvement. In addition, the results of the image processing algorithm were sent via USB port using a USB to serial converter. Due to the limitations of the converter used, baud rates above 38400bps could not be used. Given this baud rate, it took about 8ms to send the results via serial the port. This time could be reduced to 1ms if a higher quality converter were used. These two suggestions would result in a total of 25ms time delay improvement, which would reduce the time delay of the proposed scheme from 35ms to 10ms. The decrease in the time delay would decrease the oscillations, thus further increase the robustness of the proposed scheme.

6. **Conclusion.** In this study, an inverted pendulum system was controlled using visual feedback. An LQR based FSF control method was employed. The FSF method was implemented with Dspace DS1103 real time controller. The vision and the control part of the system were developed separately. In order to test robustness of the system, external forces and visual disturbances (similar rod or other objects) were applied to the system. Based on the experiments, the control algorithm of the pendulum system was found to be very robust. The performance of the system with visual feedback was found to be almost similar to the one with encoder feedback. An effective and simple estimation algorithm was also developed to reduce time delay of the image processing algorithm from 60ms to 35ms. In the final system, the amount of steady oscillations in the pendulum angle was obtained to be only 0.2° while the pendulum was stabilized at its equilibrium point.

REFERENCES

[1] Y. Morita and H. Wakuya, Online feedback error learning control for an inverted pendulum, *International Journal of Innovative Computing, Information and Control*, vol.5, no.10(B), pp.3565-3572, 2009.

[2] S. Kizir, Z. Bingul and C. Oysu, Fuzzy control of a real time inverted pendulum system, *Journal of Intelligent & Fuzzy Systems*, vol.21, no.1-2, pp.121-133, 2010.

[3] M. E. Magana and F. Holzapfel, Fuzzy-logic control of an inverted pendulum with vision feedback, *IEEE Transactions on Education*, vol.41, no.2, pp.165-170, 1998.

[4] E. S. Espinoza-Quesada and L. E. Ramos-Velasco, Visual servoing for an inverted pendulum using a digital signal processor, *Proc. of IEEE International Symposium on Signal Processing and Information Technology*, Vancouver, Canada, pp.76-80, 2006.

[5] H. Wang, A. Chamroo, C. Vasseur and V. Koncar, Hybrid control for vision based cart-inverted pendulum system, *Proc. of American Control Conference*, Seattle, Washington, USA, pp.3845-3850, 2008.

[6] M. Stuflesser and M. Brandner, Vision-based control of an inverted pendulum using cascaded particle filters, *Proc. of the IEEE Instrumentation and Measurement Technology Conference*, Victoria, Canada, pp.2097-2102, 2008.

[7] Y. Tu and M. Ho, Design and implementation of DSP and FPGA-based robust visual servoing control of an inverted pendulum, *Proc. of IEEE International Conference on Control Applications*, Yokohama, Japan, pp.83-88, 2010.

[8] H. Wang, A. Chamroo, C. Vasseur and V. Koncar, Stabilization of a 2-DOF inverted pendulum by a low cost visual feedback, *Proc. of American Control Conference*, Seattle, Washington, USA, pp.3851-3856, 2008.

[9] P. Pannil, K. Tirasesth, P. Ukakimaparn and T. Trisuwannawat, Derivative state constrained optimal H2 control for unstable systems, *International Journal of Innovative Computing, Information and Control*, vol.5, no.10(B), pp.3541-3552, 2009.

[10] N. S. Nise, *Control Systems Engineering*, John Wiley & Sons, New York, 2004.

[11] R. C. Gonzalez and R. E. Woods, *Digital Image Processing*, 2nd Edition, Prentice Hall, New Jersey, 2002.